

GA-A23509

INTEGRATED NEUTRAL BEAM MEASUREMENTS IN A TOKAMAK ENVIRONMENT

by
D.M. THOMAS

SEPTEMBER 2000

DISCLAIMER

This report was prepared as an account of work sponsored by an agency of the United States Government. Neither the United States Government nor any agency thereof, nor any of their employees, makes any warranty, express or implied, or assumes any legal liability or responsibility for the accuracy, completeness, or usefulness of any information, apparatus, product, or process disclosed, or represents that its use would not infringe privately owned rights. Reference herein to any specific commercial product, process, or service by trade name, trademark, manufacturer, or otherwise, does not necessarily constitute or imply its endorsement, recommendation, or favoring by the United States Government or any agency thereof. The views and opinions of authors expressed herein do not necessarily state or reflect those of the United States Government or any agency thereof.

INTEGRATED NEUTRAL BEAM MEASUREMENTS IN A TOKAMAK ENVIRONMENT

by

D.M. THOMAS

This is a preprint of a paper to be presented at the International Conference on the Application of Accelerators in Research and Industry, November 1-4, 2000, Denton, Texas and to be published in the Proceedings.

Work supported by
the U.S. Department of Energy under
Contract No. DE-AC03-99ER54463

GA PROJECT 30033
SEPTEMBER 2000

ABSTRACT

Tokamaks are, in many respects, the most promising avenue for the development of fusion power. The continual improvement in the performance of these devices and our understanding of them is due in great measure to the development of accurate plasma diagnostics. Many of the most crucial measurements required to assess our progress on these experiments are based in one way or another upon collisional interactions of injected neutral beams with the plasma. These measurements include such fundamental parameters as the ion temperature, rotation, and density profiles, electric and magnetic field structure, and local studies of the plasma turbulent transport. Maximizing the obtained information for a given geometry of plasma, beams, and possible viewchords represents an interesting challenge to the experimentalist. Advances in detector and analysis techniques allow us to take full advantage of the beam/plasma emission for these measurements.

1. INTRODUCTION

In the quest for fusion power, improving the performance of stable magnetic confinement schemes has been a key scientific issue. The most well developed scheme, the tokamak, has led the charge in this area. Recent progress on heating and controlling fusion-grade plasmas using the tokamak concept has led to the achievement of near scientific breakeven (Fusion power/input power \sim 1) in several experiments worldwide, albeit on a transient basis. Our challenge for the future is to maintain and improve these performance levels on a steady-state (and ultimately economical) basis.

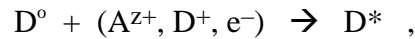
A crucial element of this progress has been the implementation of plasma diagnostics to measure various plasma parameters in situ. These measurements have become more and more complex as the plasma environment becomes more hostile (radiation, remote sightlines, larger dimensions, hotter plasmas). In particular, the recent development of the highest performance “advanced” tokamak modes has relied on the careful crafting of the plasma pressure and rotation profiles, requiring good internal measurements of these parameters with high spatial temporal resolution. Fortunately, the high intensity neutral beams typically used for heating these plasmas represent a powerful tool in this regard. By properly collecting and interpreting the optical emission resulting from beam-plasma collisions, in many cases we can infer the relevant plasma behavior without the need for material contact with the plasma. These techniques, and the relevant cross section work necessary to properly interpret the measurements, have been utilized on essentially all devices having heating beams or dedicated diagnostic neutral beams. In this paper, we will briefly review some of these techniques as they are employed on the DIII-D tokamak experiment.

2. MEASUREMENTS USING BEAM-PLASMA COLLISIONS ON DIII-D

The DIII-D program employs eight neutral deuterium beams for plasma heating, permitting over 20 MW of injected power per shot [1]. The beams are typically 40 keV/AMU $^2D^0$, but can easily be run down to ~30 keV/AMU if necessary. A versatile beam control system permits modulation of each of the beams down to 5 ms pulse widths. The production of diatomic and triatomic deuterium ions in the ion source results in full, half, and third energy components in the neutral beam after acceleration and neutralization. The species mix injected into DIII-D at optimum perveance typically results in initial beam densities of 1×10^{15} atoms/m³ in the beam footprint of 0.26×0.14 m (height x width). The typical 1/e divergence angle for the beams is 0.66° in the horizontal plane and 1.30° in the vertical plane at optimum perveance [2].

We may distinguish between possible measurements based on beam-plasma collisions as being due to either:

1. Beam excitation processes



where the subsequent decay emission gives information about the beam atoms and their environment; or

2. Charge transfer processes



where the decay emission is now indicative of the parent ion population. Although not discussed in this paper, observation of the neutral particle emission from reactions of this type for the case $z=1$ can also be used to study the distribution function of the parent ion, using neutral particle analysis at the periphery of the plasma.

3. CHARGE EXCHANGE SPECTROSCOPY

On DIII–D, detailed measurements of impurity ion behavior (heating, confinement, and transport) are made using reactions of Type 2 above [3]. A rather extensive set of viewing chords (24 tangential and 16 vertical) have been installed and collimated to collect light from ~6–12 mm spot sizes. These views are arranged so as to be as tangent to the magnetic flux surfaces as possible at the point of beam intersection. This results in the maximum spatial resolution given the finite beam dimensions. The coverage in the edge region is especially good (chord spacing ~6 mm) in order to isolate fine scale structure in the edge. The progressive development of high quantum efficiency CCD detectors, efficient grating spectrometers, and high-speed readout electronics permits us to extract spectral information on every chord over the range 300–1100 nm with gating times down to 0.32 ms [4,5]. The resulting spectra are fit with a nonlinear least-squares fitting routine to identify the various peaks. Extensive spatial, wavelength, and intensity calibrations of all channels are conducted on a routine basis. These calibrations permit us to extract the impurity ion density, velocity, and temperature profiles from the amplitude, shift, and width of the spectral lines. To obtain absolute ion density profiles, one also needs to know the local beam density, species mix, and energy-dependent charge transfer cross sections. These basic measurements then let us infer impurity ion pressure profiles. Since the inner wall of the DIII–D vacuum vessel is lined with carbon tiles, our workhorse transition for these measurements is the C VI ($\Delta n = 8 \rightarrow 7$) transition at 529.05 nm, resulting from the recombination of fully stripped carbon ions with the beam atoms.

Figure 1 demonstrates the quality of the present system, where we are able follow the formation of a transport barrier both in the core [internal transport barrier (ITB)] and edge [high confinement (H–mode)] of a high performance DIII–D discharge. The data quality is such that we can perform rigorous tests of theories dealing with formation of these enhanced confinement regimes. In this regard, the precise determination of the poloidal and toroidal velocity profiles is particularly valuable as it allows us to infer the intrinsic radial electric field structure using force balance arguments. We now believe that it is the shear in the electric field (or more properly, the shear in $E \times B$ flow) that plays a pivotal role in the suppression of turbulence and the improved confinement behavior [6].

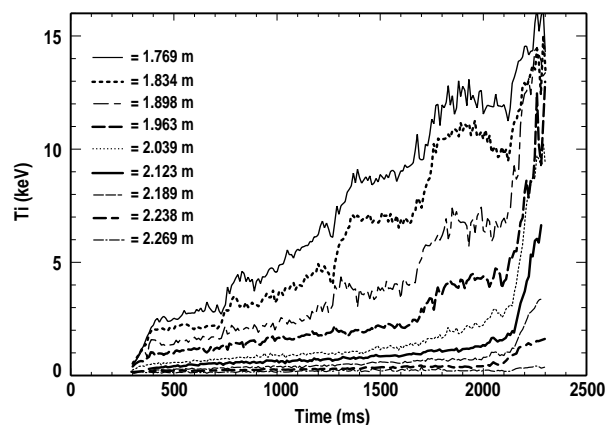


Fig. 1. C VI ion temperature measurements on DIII–D, showing internal and external transport barriers.

4. BEAM EMISSION SPECTROSCOPY

Improvements in detector technology have also benefited observations of beam emission reactions of Type 1. Because the beam emission is proportional to excitation rate, and the rate itself is relatively insensitive to temperature in the energy range of interest, variations in the detected emission rate may be related directly to the underlying fluctuations in the plasma density [7–9]. By viewing the beam at a non-normal angle, the Doppler-shifted D_α beam emission may be distinguished spectroscopically from the large thermal D_α emission along the line of sight. Because of the large Doppler shifts obtained on DIII–D, we can use interference filters for this purpose rather than grating spectrometers, resulting in vastly improved light levels. Large collection optics and a two-dimensional array of fibers allow us to measure radially and poloidally localized density fluctuations with high time resolution (1 MHz digitization rate) and high spatial resolution (~ 1 cm resolution). This allows us to analyze the turbulent state of the plasma in great detail. An example is shown in Fig. 2, where neon was puffed into the periphery of the plasma in an attempt to suppress turbulence and improve confinement [10].

For this data, 32 spatial channels were deployed to examine the outer third of the plasma minor radius, with one 16-channel radial array and two poloidal arrays being used. Plotted is the relative density fluctuation power spectra for a neon puff shot and reference shot, before and after the neon injection occurs. The wavenumber listed is determined experimentally by the channel separation. We note two distinct effects of the neon injection: the overall power of the fluctuation spectrum is substantially reduced, with preferential lowering of the higher frequencies, corresponding to preferential suppression of the higher- k turbulent modes. These effects occur on the same timescale as do improvements in the global plasma confinement. These techniques have been extended to provide two-dimensional images of the turbulence [11].

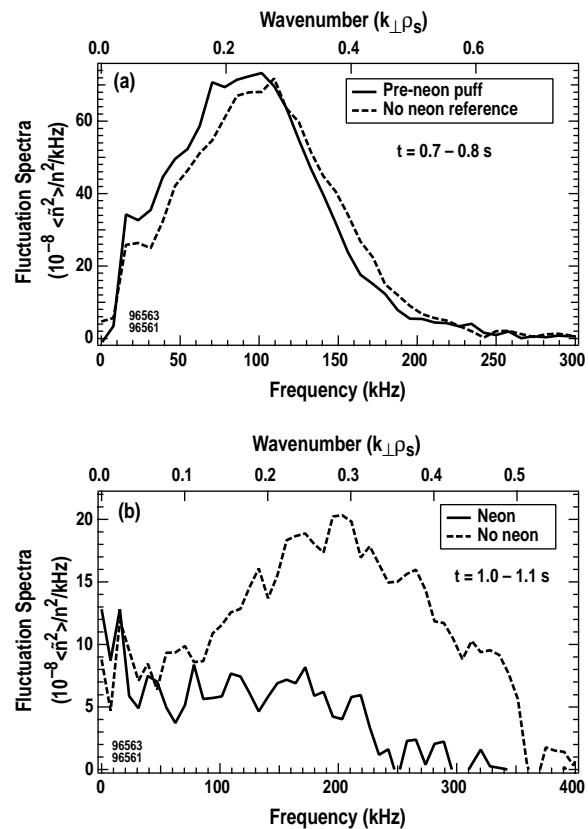


Fig. 2. BES power spectra with and without N_e puff [10].

5. MOTIONAL STARK EFFECT (MSE) SPECTROSCOPY

Performing more detailed spectroscopy on the beam emission yields additional information about the plasma. The neutral deuterium beam atoms are transiting a large magnetic field $\mathbf{B}=\mathbf{B}_{\text{tor}}+\mathbf{B}_{\text{pol}}$ as they enter the plasma. Because of the strong motional electric field ($\mathbf{E}=\mathbf{v}\times\mathbf{B}$) produced in the rest frame of the beam atoms, the D_{α} line is actually split into orthogonally polarized components (σ,π) by the Stark effect. When viewed in a direction perpendicular to \mathbf{E} , the σ and π components are polarized perpendicular and parallel to the direction of the electric field, respectively. The emission of one of the components is then polarization analyzed to determine the pitch angle at an ($\mathbf{B}_{\text{pol}}/\mathbf{B}_{\text{tor}}$) of the local magnetic field. From this profile, one can then infer details about the internal current distribution, a critical element of plasma stability [12,13]. In order to utilize this effect, one needs sufficient perpendicular beam velocity $\mathbf{v}\times\mathbf{B}$ to separate the σ and π lines, as well as viewing tangent to \mathbf{B} (to achieve good spatial resolution) and somewhat tangent to \mathbf{v} (to achieve sufficient Doppler separation of the full, half, and third energy components from the thermal background). On DIII-D, we have three separate viewing geometries to attempt to satisfy these requirements [14].

The specifics of the current profile distribution are extremely important for the development and stabilization of high-performance plasmas. Coupled with a magnetic equilibrium reconstruction code, the MSE measurements have crucially improved both our understanding of plasma stability and confinement as well as our ability to create new regimes of plasma performance.

6. LITHIUM BEAM ZEEMAN SPECTROSCOPY

One limitation of MSE becomes apparent in studies of H-mode edge plasmas. The large intrinsic electric fields found in these plasmas causes Stark splitting effects which are indistinguishable from the MSE, leading to a superposition of magnetic and electric field effects and precluding an unambiguous determination of B_{pol} from MSE alone [15,16]. As is shown in Fig. 3, a set of radial MSE views was implemented to mitigate this E_r effect, but the radial resolution of these channels is insufficient to examine fine scale structures in the edge. Simultaneous observation using CER to identify the E_r at the same location helps somewhat in this regard. To improve the precision of the edge magnetic field determination, we are deploying an atomic lithium beam on DIII-D [17].

The lithium 670 nm 2S-2P resonance line is split by the Zeeman effect, with the π and σ lines exhibiting similar polarization behavior as utilized in MSE, but referenced to the local B . Because this transition has negligible Stark splitting, the use of this line eliminates the electric/magnetic ambiguity. Also, the type of source utilized creates no half- and third-energy components in the beam. Finally, because the cross section for collisional excitation is so large ($\sim 500 \times D_{\alpha}$), we can utilize a very small beam, permitting very fine spatial resolution (Fig. 4). The key to successfully making this measurement is handling the somewhat smaller spectral splitting ($\sim 10\times$) relative to MSE measurement, requiring much better spectral resolution. This results in a conflict with light collection efficiency and the possible time resolution. Additionally, because of the enhanced ionization/charge transfer cross sections for Li^0 , beam penetration is an issue and the measurement is only feasible in the edge plasma region.

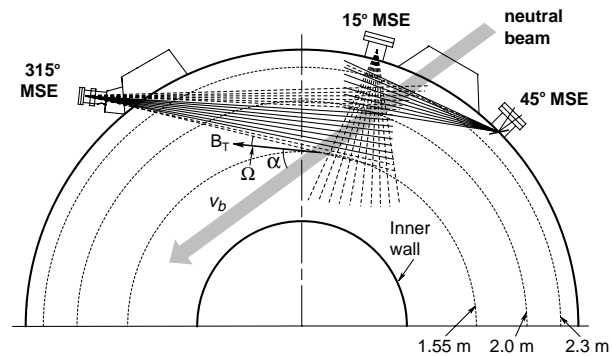


Fig. 3. MSE views on DIII-D [14].

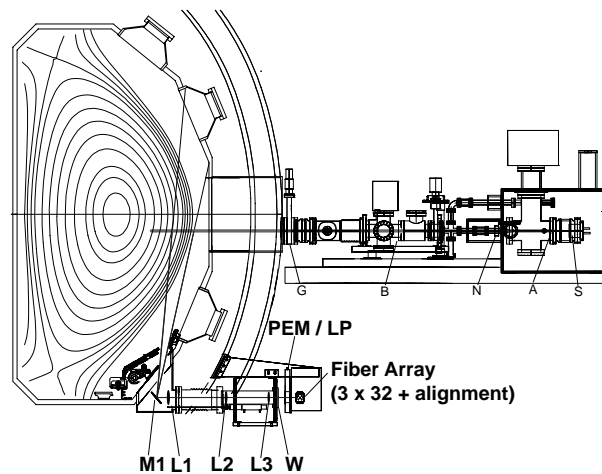


Fig. 4. Lithium beam system on DIII-D showing accelerator and optical system [17].

7. CONCLUSION

Tokamak diagnostics based on beam-plasma collisions provide a variety of unique information about the interior of fusion grade plasma devices. They serve a vital role for improving our understanding of these devices and help in assessing the ultimate prospects of the tokamak as a potential power source.

8. ACKNOWLEDGMENTS

The measurements presented here represent just a small fraction of the substantial contributions made on beam-based diagnostics on DIII-D by General Atomics, the University of Wisconsin, and Lawrence Livermore National Laboratory plasma diagnostic groups. I would also like to thank the DIII-D Neutral Beams Group for providing the specific information on the operation and performance parameters for the DIII-D heating neutral beams. This work was supported by U.S. DOE Contract No. DE-AC03-99ER54463.

9. REFERENCES

1. Hong, R., *et al.*, “Enhancement of DIII–D Neutral Beam System for Higher Performance,” Proc. 17th Symp. on Fusion Technol., Rome, 1992.
2. Chiu, H., *et al.*, “Measurement of Neutral Beam Profiles at DIII–D,” Proc. 13th Top. Mtg. Technol. Fusion Energy, Nashville, 1998.
3. Gohil, P., *et al.*, “The Charge Exchange Recombination Diagnostic System on the DIII–D Tokamak,” Proc. 14th IEEE/NPSS Symp. on Fusion Engineering, California, 1991, Vol. 2 (IEEE, New Jersey, 1992) p. 1199.
4. Thomas, D.M., *et al.*, *Rev. Sci. Instrum.* **68**, 1233 (1997).
5. Burrell, K.H., *et al.*, “Improved CCD Detectors for the Charge Exchange Spectroscopy System on the DIII–D Tokamak,” to be published in *Rev. Sci. Instrum.* (2000).
6. Burrell, K.H., *et al.*, *Phys. Plasmas* **4**, 1499 (1997).
7. Fonck, R.J., Duperrex, P.A., Paul, S.F., *Rev. Sci. Instrum.* **61**, 3487 (1990).
8. Durst, R.D., Fonck, R.J., Cosby, G., *et al.*, *Rev. Sci. Instrum.* **63**, 4907 (1992).
9. McKee, G., *et al.*, *Rev. Sci. Instrum.* **70**, 913 (1999).
10. McKee, G., *et al.*, *Phys. Rev. Lett.* **84**(9), 1922 (2000).
11. Fenzi, C., *et al.*, “2D Turbulent Imaging in DIII–D via Beam Emission Spectroscopy,” to be published in *Rev. Sci. Instrum.* (2000).
12. Levinton, F.M., *et al.*, *Phys. Rev. Lett.* **63**, 2060 (1989).
13. Wroblewski, D., *et al.*, *Rev. Sci. Instrum.* **61**, 3552 (1990).
14. Rice, B.W., *et al.*, *Rev. Sci. Instrum.* **70**, 815 (1998).
15. Rice, B.W., *et al.*, *Nucl. Fusion* **37**, 517 (1997).
16. Zarnstorff, M.C., *et al.*, *Phys. Plasmas* **4**, 1097 (1997).
17. Thomas, D.M., *et al.*, “Prospects for Edge Current Density Determination using LIBEAM on DIII–D,” to be published in *Rev. Sci. Instrum.* (2000).